# Numerical Analysis of Multilayer Geosynthetic-Reinforced Bed Over Stone Columns-Improved Soft Clay


**Mobin Afzalirad, Mehran Naghizadehrokni, Martin Ziegler and Mojtaba Razaghnia**

**Abstract** Installation of stone columns is recognized as a usual procedure for the treatment for soft clay soils. In the current research, three-dimensional finite-element analyses were performed to simulate the behavior of multilayer geosynthetic-reinforced granular bed over stone column-reinforced soft soil using the ABAQUS. An extensive research was conducted for better understanding of the mechanism of load transfer in ordinary stone columns (OSCs) and geosynthetic-encased columns (GECs) installed under a concrete foundation. Parametric studies were also carried out to investigate the effects of factors such as hardness of the geosynthetic encasement and the region replacement proportion on the overall behaviour of the GECs group. The results designated that utilizing of more than one geosynthetic reinforcement with stone columns is not so effective to reduce the maximum settlement. But, a multilayer reinforcement system is efficient to decrease the maximum settlement when stone columns are not used. It was also shown that there is a large growth in the amount of stress concentration proportion with the presence of geosynthetic reinforcement in comparison with the amount when there is no geosynthetic reinforcement present.

**Keywords** Stone column · Geosynthetic-Reinforced bed · Soft soil
Finite-element method · 3D analysis

## 1 Introduction

Large segments, particularly along the beach, are covered with thick soft marine clay deposits which have very low shear strength and high compressibility. Stone columns, one of the most commonly used soil improvement technique, have been

M. Afzalirad · M. Razaghnia
Institute of Civil Engineering, University of Azad, Qaemshahr, Iran

M. Naghizadehrokni (✉) · M. Ziegler
RWTH Aachen University, Geotechnical Engineering, Aachen, Germany
e-mail: Naghizadehrokni@geotechnik.rwth-aachen.de



B. Pradhan (ed.), *GCEC 2017*, Lecture Notes in Civil Engineering 9,
https://doi.org/10.1007/978-981-10-8016-6_12

utilized throughout the world to enhance the bearing capacity of the soft soils and decrease the settlement of superstructures constructed on them. Utilizing the stone columns also increases the rate of the consolidation of the soft clay.

The stone column technique was adopted in European Countries in the early 1960s. Stone columns in compressive loads fail in different modes, such as bulging [1], general shear failure [2], and sliding [3]. But, the most usual failure mode for stone columns in soft clays is bulging [4].

A granular layer of sand or gravel, 0.3 m or more in thickness, is usually placed over the top of the stone columns for catering a drainage route and spread the stresses coming from the superstructures. Selecting a proper diameter, stiffness, and spacing of the stone columns is very important to improve an existing soft soil. Studies have shown that maximum settlement decreases as the stiffness of the stone column raises, however differential settlement which is the settlement difference between the center of the stone columns and the mid-span of the column spacing, increases [5, 6]. Thus, a suitable level of stiffness must be utilized to gain an optimum amount of the maximum and the differential settlement of the improved ground. It has been further seen that the rate of the stabilization of the soft soil increases as the stiffness of the stone column increases [7]. The maximum and differential settlement increases as the spacing-to-diameter ratio increases [5], whereas the rate of consolidation decreases as this ratio increases.

Horizontal geosynthetic-reinforcement sheets can be used in the granular columns to increase the load-carrying capacity as well as decrease the bulging of the columns [4, 8]. Van Impe proposed the concept of covering the stone column by wrapping with geotextile in the year 1985 [9]. Geosynthetic encasement can also be used to extend the use of stone columns for extremely soft soil condition [10–14]. The first projects started successfully in Germany around 1995 [15].

The granular bed can be further reinforced with the geogrid to boost the load-carrying capacity and decrease the settlement of the stone column-improved soft clay. Han and Gabr [8] carried out a numerical analysis of geosynthetic-reinforced and pile-supported earth platforms over soft soil. Based on lumped parameter modeling approach, models have been expanded for single layer [5, 16]. Deb et al. [17] have been done a laboratory model test on single-stone column to study the effect of reinforcement diameter and thickness response, bearing volume and construction of the stone column. The published literature on the performance of reinforced granular fill over soft soil with stone columns group is limited.

In the present study, the results of 3D numerical analyses of different aspects of the performance of multilayer geosynthetic-reinforced granular bed over stone column-reinforced soft soil were presented using the finite-element program ABAQUS. The calibration of the methods utilized in the numerical analyses was performed by modeling the experimental results presented by Ambily and Gandhi [18]. A comprehensive study was carried out to better understanding the load-transfer mechanism of a group of Geosynthetic Encased Columns (GECs) and the multilayer geosynthetic-reinforced granular bed over stone column-reinforced. The results of the numerical study conducted for the effect of multilayer

geosynthetic-reinforced granular fill over soft soil with stone columns on settlement response, bearing capacity and bulging of the stone column were reported.

## 2 Validation of Finite-Element Model

In order to calibrate the numerical procedure used in the present research, the settlement results gained from the current finite-element analyses were compared with the experimental results presented by Ambily and Gandhi [18]. The model tests were performed on a group of seven stone columns arranged in a triangular pattern as illustrated in Fig. 1. The diameter of the stone columns utilized in the model test was 100 mm and spacing between the stone columns was taken as 300 mm. The diameter was 835 mm and load was applied through a 16 mm thick mild steel plate with stiffeners to ensure negligible constructional deformation. A 30 mm thick sand bed was located between the stone columns and the footing. The length of the stone columns was equal to the depth of the soft soil (450 mm). The clay, sand, and stones material behaviors were simulated using Mohr–Coulomb's criterion. The finite-element mesh was expanded utilizing eight-node linear brick elements for the stone columns, clay, and sand, displayed in Fig. 2. At the bottom boundary of the finite-element mesh, the displacements are set to zero in the z direction. The displacements in the $x$ and $y$ directions were set to zero on the circumferential boundary of the soft soil zone. In following model test, footing was loaded up to 4.6 mm settlement. Figure 3 compares the results obtained from the model test and based on the current FEM analysis, which matches well. This comparison shows that the predicted values from the settlement using the present analysis have acceptable correspondence with the experimental results.

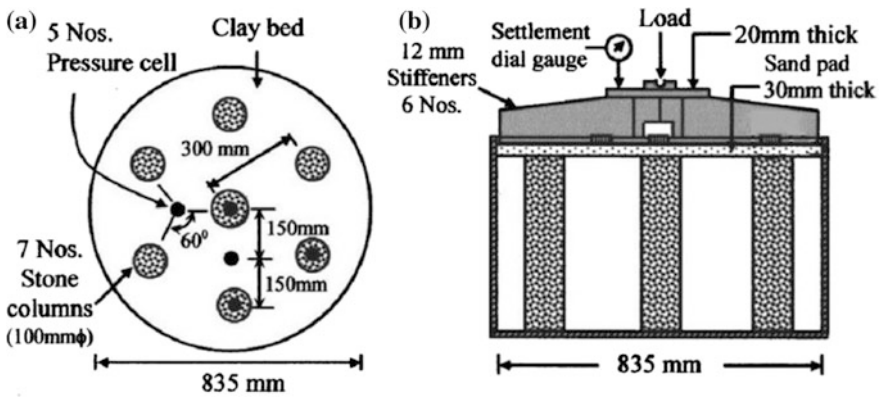


**Fig. 1** Group test arrangement: **a** plan view; and **b** section of test tank Ambily and Gandhi [18]

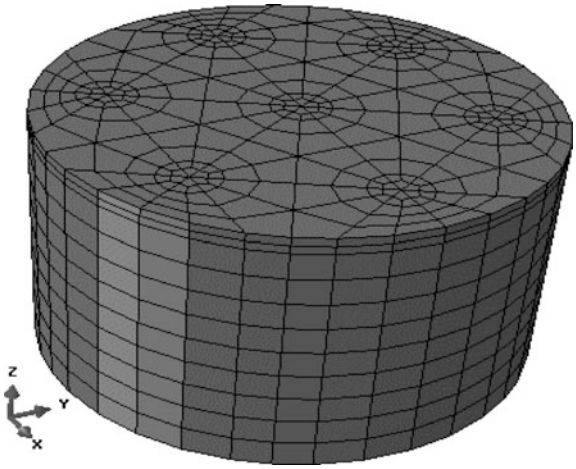


**Fig. 2** Finite-element mesh used for the calibration analyses

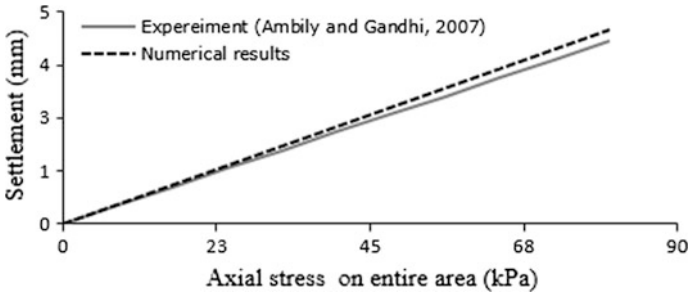


**Fig. 3** Comparison of maximum settlements for the calibration analyses

## *2.1 Numerical Modeling*

Finite-element analyses were carried out by the ABAQUS Program. Since there are two planes of symmetry in the zone of interest, it was only vital to numerically model the behavior of the system over a quarter of the domain. In all of the numerical analyses that were carried out, the thickness of the soft soil and length of the stone columns were assumed to be 10 m. A 300 kPa surcharge pressure was applied in 100 increments on the stone columns group through a 1 m thick, linear-elastic concrete foundation. A multilayer geosynthetic-reinforced granular fill resting on soft soil with stone columns can be seen in Fig. 4 [19].

At the bottom boundary of the finite-element mesh, the displacements were set to zero in the z direction. The displacements in the *x* and *y* directions were set to zero on the circumferential boundary of the soft soil zone. On the planes of symmetry,

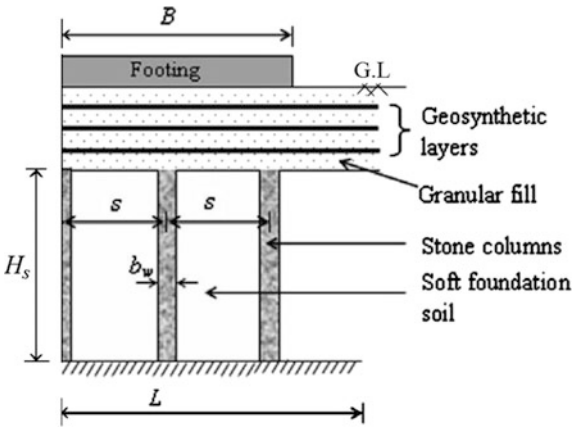


**Fig. 4** Multilayer geosynthetic-reinforced granular fill resting over soil with stone columns

normal displacement was restricted. The diameter of geogrid reinforcement was chosen as two times the diameter of the footing.

Figure 5 shows a typical finite-element mesh used in the analyses. The finite-element mesh used in the numerical simulations was developed using eight-node Linear Brick elements for both the stone column, sand and soft soil. For constitutive modeling, the clay soil was represented by the modified Cam clay (MCC) material while the linear-elastic, perfectly plastic model (the Mohr–Coulomb failure criterion) was used to model the crushed stone, and sand. It should be noted that the MCC parameters considered in this study were inferred from the geotechnical parameters of soft soils encountered in a recent soft ground improvement project [20]. The Mohr–Coulomb parameters used in the numerical analyses were based on the material properties that Ambily and Gandhi [18] used in their tests, and are presented in Table 1.

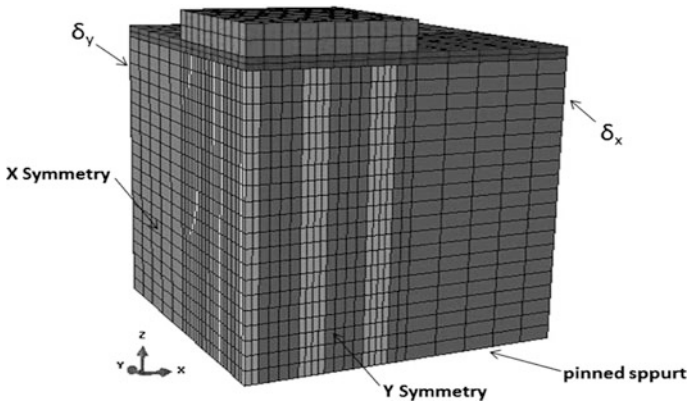


**Fig. 5** Typical finite-element mesh used in the analyses

**Table 1** Material properties used in the numerical models

| Material properties | Stone column | Soft soil | Sand |
|---|---|---|---|
| Sat. unit weight (kN/m$^3$) | – | 17 | – |
| Dry. unit weight (kN/m$^3$) | 16.62 | – | 15.50 |
| Young's modulus (kPa) | 55,000 | – | 20,000 |
| Poisson's ratio | 0.3 | 0.3 | 0.3 |
| Cohesion (kPa) | 0 | – | 0 |
| Friction angle (deg) | 43 | – | 10 |
| Dilation angle (deg) | 10 | – | 4 |
| Critical state stress ratio ($M$) | – | 1.3 | – |
| logarithmic hardening constant for plasticity ($\lambda$) | – | 0.3 | – |
| logarithmic bulk modulus for elastic material behavior ($\kappa$) | – | 0.02 | – |
| Initial void ratio ($eo$) | 0.62 | 1.5 | 0.74 |

The geosynthetic was modeled using four-node quadrilateral, decreased integration membrane elements. The geosynthetic was assumed to be an isotropic linear-elastic material, with an assumed Poisson's ratio of 0.3 [21]. Based upon the results of a prior comprehensive numerical study [14], to avoid adversely influencing the numerical results, and knowing that the encasement did not carry vertical (compressive) load, the "No Compression" option that is available in ABAQUS was utilized to more appropriately characterize the behavior of the geosynthetics.

Alexiew [22] documented that design values of tensile modulus ($J$) between 2000 and 4000 KN/M were required for the geosynthetic used to encase stone columns on a number of different projects. Consequently, a circumferential elastic modulus of 4000 KN/M was used in the numerical analyses. The circumferential elastic modulus ($E$) of the geosynthetic was derived from the relationship $J = Et$, where $t$ is the thickness of geosynthetic, which was assumed to be 5 mm for all of the numerical analyses performed. The various stone columns are referred to use the column numbers which are shown in Fig. 6.

## 3 Numerical Results Multilayer Geosynthetic-Reinforced Sand Bed Resting Over Soil with Stone Columns

In this section, effects of various design parameters on the performance of multilayer geosynthetic-reinforced sand bed resting over soil with stone columns installed under a concrete foundation are examined. The settlement and lateral deformation and force of stone columns obtained from the analyses were selected as representatives of the group behavior.

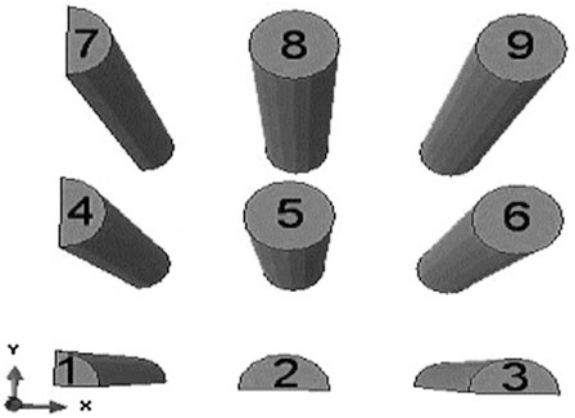


**Fig. 6** Stone column numbers used in numerical modeling

## *3.1 Load-Settlement Characteristics*

Figure 7 shows the variation of maximum settlement with load for multilayer geosynthetic-reinforced sand bed with 1 m thick over soft soil. It has been observed that if the soft soil is not improved with stone columns, the reduction of the maximum settlement at the center of the loaded region as compared to the unimproved soil is 16, 22, and 27% as the number of geosynthetic layers increases from 1 to 3 respectively. The maximum settlement reduction is 37% if only stone columns are used. Thus, it can be said that the use of multilayer reinforcement system is effective to reduce the maximum settlement when stone columns are not used.

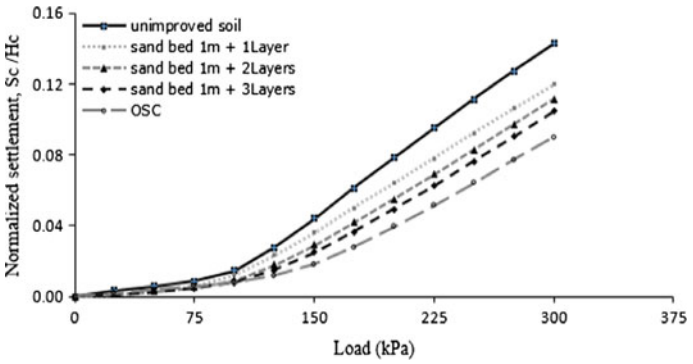


**Fig. 7** Load-settlement characteristics of reinforced sand bed layers

### 3.2 *Lateral Deflections of Stone Column*

Figure 8 which is contour lateral displacement is shown the results from the full 3D analyses for a group of OSC. As it can be seen, the incidence of failure mechanisms is clearly visible and the maximum lateral displacement in the stone columns, the columns of the upper elements circumferential ring, occurs. So the pattern lateral displacement of the stone columns is important. In the field, most constructed stone columns have equal ratios of length-to-diameter and a bulging failure usually develops depending on whether the tip of the column is floating in soft soil or resting on a firm bearing layer [23].

The effect of unreinforced and geosynthetic-reinforced sand bed placed over stone column on bulging behavior of the column has been studied. The lateral deflection of column number 25 obtained from the analyzed models are presented in Fig. 9. In the case of only stone column-improved soft clay, a maximum bulge of 145 mm has been observed at a depth of 3 m from top of stone column. As compared to the only stone column-improved soil, 5.5% reduction in maximum bulge diameter of the stone column has been observed when sand bed is placed over the stone column-improved soft clay. Additional 20% reduction in maximum bulge diameter has been observed when geosynthetic reinforcement is placed within the sand bed. It can be concluded that the maximum bulge diameter of stone column reduces and the depth of bulge increases with the application of sand bed. Inclusion of geosynthetic reinforcement further reduces the bulge diameter and increases the bulge depth.

Shahu et al. [24] shows that adequate thickness of granular mat reduces the load carried by granular pile both at the top and bottom and helps to reduce the failure of the granular pile due to bulging of the pile. Very high stress concentration has been observed near the top of the columns, which causes high bulging. However, when

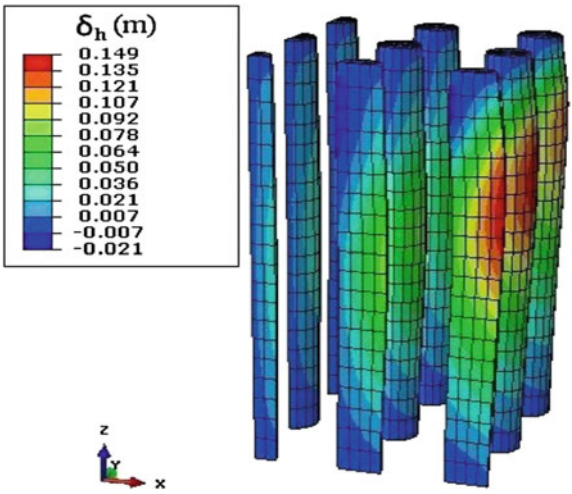


**Fig. 8** Contour plots lateral displacement of stone columns

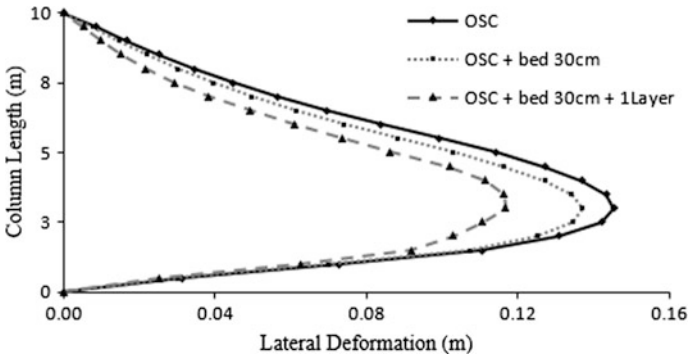


**Fig. 9** Lateral deflections of the stone column 6 when soft clay has been improved with stone column alone, unreinforced and geosynthetic-reinforced sand bed over stone column-improved soft clay

sand bed is placed over the stone column-improved soft clay, significant reduction in stress concentration on top of the column has been observed and the variation of stress concentration with depth is more uniform. Thus, placement of sand bed on top of the stone column-improved soft clay reduces the bulge diameter and increases the bulge depth of the stone column.

## *3.3 Optimal Thickness of the Geosynthetic -Reinforced Sand Bed*

Figure 10 shows the load-settlement characteristics of the geosynthetic-reinforced sand bed of different thicknesses where it is placed over stone column-improved clay. It has been observed that as the ratio of thickness of sand bed to the diameter

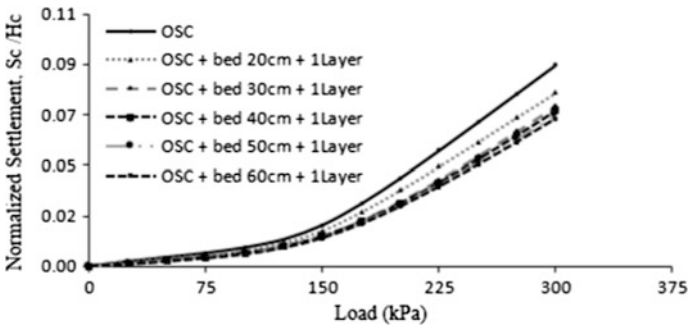


**Fig. 10** Load-settlement characteristics of reinforced sand bed of different thicknesses over stone column-improved soft clay

of the footing ($H_s/D$ ratio) increases, the load-carrying capacity also increases up to a value of 0.3. Whereas beyond this value, the load-carrying capacity decreases by increasing the thickness of the sand bed. Thus, the optimum thickness of geosynthetic-reinforced sand bed is 0.3 times the diameter of the footing.

The vertical component of the tensile force acts in the geosynthetic reinforcement partially counterbalances by the overlying soil. As a result, the vertical stress is reduced in the zone due to combined action of mobilized tension in the reinforcement and membrane action in its curvature [25–27]. However, when the sand bed thickness increases such that $H_s/D > 0.3$, a major portion of the shear failure zone of the soil is developed above the reinforcement layer and the deflection of the reinforcement also decreases [27]. This phenomenon reduces the effectiveness of the geosynthetic layer causing reduction in bearing capacity. Thus, the stone column under geosynthetic-reinforced sand bed having $H_s/D = 0.4$ produces less bearing capacity than that under geosynthetic-reinforced sand bed having $H_s/D = 0.3$. This is due to the fact that as the thickness of the reinforced sand bed increases, the deflection of the reinforcement decreases and the effectiveness of the reinforcement also decreases [17].

The effect of tensile stiffness of the geosynthetic on the settlement response has been studied for multilayer-reinforced soil. It is seen that irrespective of the number of reinforcement layer, the maximum settlement decreases (Fig. 11) as the stiffness of the geosynthetic layers increases up to the range of 4000–5000 kN/M, beyond which the rate of change in settlement is negligible. The reduction in the values of settlement is 22, 25.6, and 28% for one, two and three layers case, respectively.

## 3.4 Load Transfer

To investigate the effects of the geosynthetics-reinforced sand bed of 1, 2, and 3 reinforced layers on the end-bearing behavior, load-transfer curves of stone column

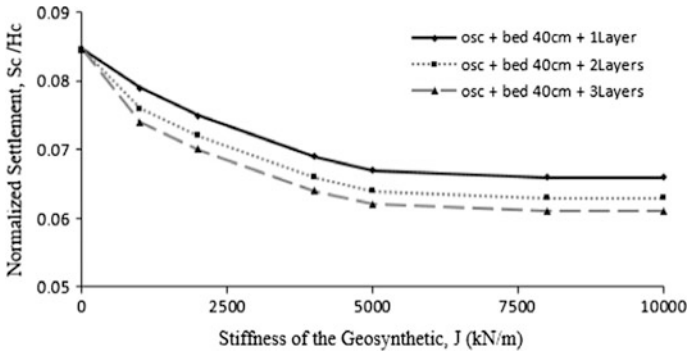


**Fig. 11** Effect of geosynthetic tensile stiffness on maximum settlement geosynthetic -reinforced sand bed over stone column-improved soft clay

at a 300 kPa surcharge pressure are shown in Figs. 12 and 13 show the load transfer of column 1 and 6, respectively. The force of columns number 1 and 6 has been increased by 116 and 112% when the soil is improved by stone columns along with unreinforced sand bed, respectively. Use of single layer geosynthetics-reinforcement with stone columns increases the value of column force at surface by 135% whereas the increment is 143 and 148% if two and three layers of geosynthetics-reinforcement are used with stone columns, respectively.

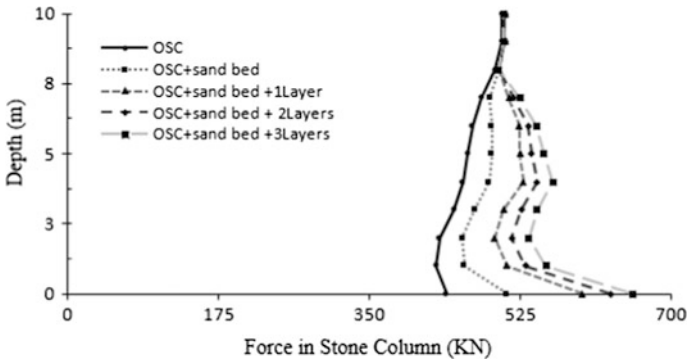


**Fig. 12** Load-transfer curves of column 1 for geosynthetic-reinforced sand bed over stone column-improved soft clay

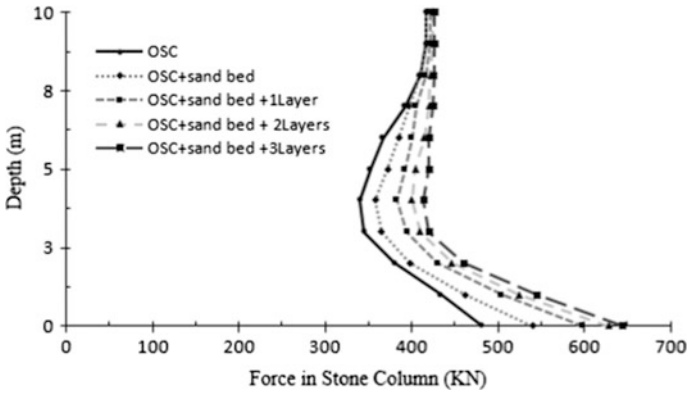


**Fig. 13** Load-transfer curves of column 6 for geosynthetic-reinforced sand bed over stone column-improved soft clay

## 4 Mechanism of GECs Behavior

Mechanisms governing GECs behavior (in relation to the influencing factors) are presented in the following sections.

### *4.1 Load Transfer*

In stone column-reinforced ground, stress concentration occurs in stone columns due to the higher relative stiffness of the column to soil, the degree of which can be quantified using the stress concentration ratio (SCR), which is defined as the ratio of the stress on the stone column, $\sigma'_{v,\mathrm{SC}}$, to that on the soil, $\sigma'_{v,\mathrm{cl}}$. As the degree of load transfer between the column and the soil depends largely on the modulus ratio between the stone column and the soil, the SCR is thus expected to be larger for a GECs than for a OSCs.

Figure 14 shows the vertical stress in the stone column-normalized settlement ($S_\mathrm{c}/H_\mathrm{c}$) displacement response for both a GECs and OSCs. Increased encasement stiffness also increases the vertical stress in the stone column $\sigma'_{v,\mathrm{SC}}$, such that at a settlement of 390 mm, the mobilized vertical stress on top of the GECs with $J$ = 10,000 KN/M is 2.4 times greater than that of OSCs.

The use of encasement can noticeably enhance the load-carrying capacity of OSCs (Fig. 12), it is instructive to more comprehensively study the load-transfer mechanism of both OSCs and GECs.

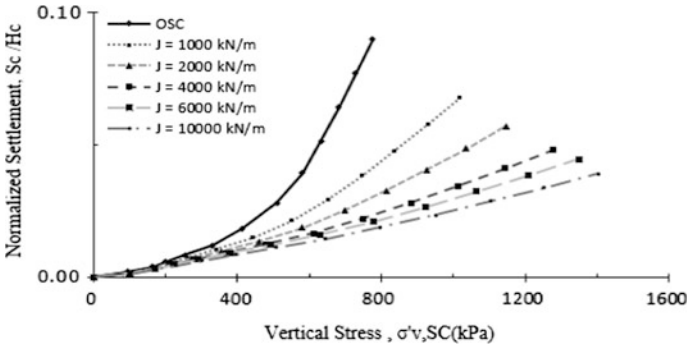


**Fig. 14** Effect of encasement on vertical effective stress in stone column

## 4.2 Force in Stone Column

The end-bearing capacity of columns is another component that should be considered when the overall load-transfer behavior of these systems is studied. To investigate the effects of column encasement on the end-bearing behavior, load-transfer curves of an OSC and GECs at a 300 kPa surcharge pressure are shown in Figs. 15 and 16. Figures 15 and 16 show the load transfer of column 1 and 6, respectively.

The distributions of computed column force with depth are presented in Fig. 15. The column force increased with depth until a maximum value of 720 kN was achieved at about mid-depth. This is due to negative drag-down from the surrounding clay that tends to settle more than that of the stone column.

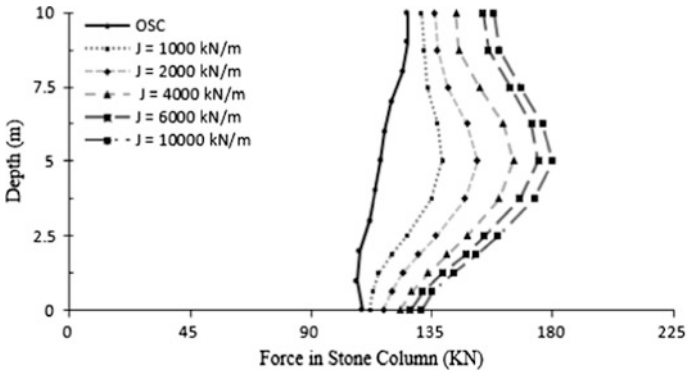


**Fig. 15** Load-transfer curves of stone column 1 obtained from models with various encasement stiffness

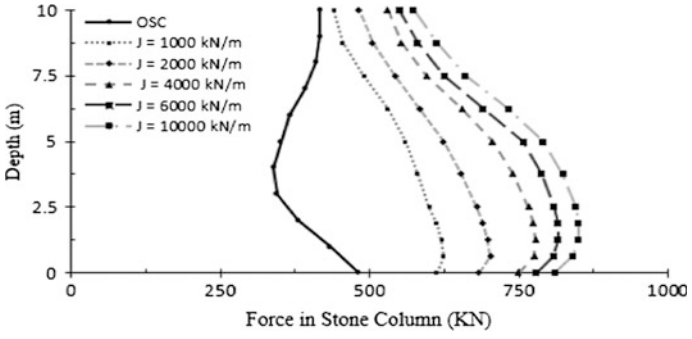


**Fig. 16** Load-transfer curves of stone column 6 obtained from models with various encasement stiffness

From Fig. 16, it can be seen that both the OSCs and GECs are primarily end-bearing columns as 86 and 70% of the loads applied at the ground surface are transferred to the tip of the columns, respectively. As shown in Fig. 16, the amount of load transferred to the tip of the GECs is much greater than that of the OSCs at a given settlement, because the encasement makes the GECs a stronger and more rigid element.

## 4.3 Settlement

These results demonstrate that the geosynthetic encasement can significantly reduce the settlement of the soft ground by decreasing the degree of surcharge load transferred to the clay layer and increasing the stiffness of the stone column.

Stone column encasement also increases the stiffness of the stone column-clay composite ground. Figure 17 shows the variations of surcharge pressure ($P_{sur}$)-normalized settlement ($S_c/H_c$) relationships for different values of encasement stiffness. Note that $S_c$ represents the settlement at the top of GECs. As one would expect, the slope of $P_{sur} - S_c/H_c$ curve, $K$, representing the stiffness of the GECs-reinforced ground, increases with increasing $J$, indicating that the stiffness of the GECs-reinforced ground also increases as the encasement stiffness increases. For example, $K$ increases from 3350 kPa for the OSC to 7672 kPa for the GECs with $J$ = 10,000 kN/M, demonstrating approximately a 230% increase in the capacity for the GECs-reinforced ground.

## 4.4 Lateral Deflection

Figures 18 and 19 show the lateral deflections ($\delta_h$) of column 6 and the associated geosynthetic hoop strains ($\varepsilon_g$), respectively, for different values of encasement

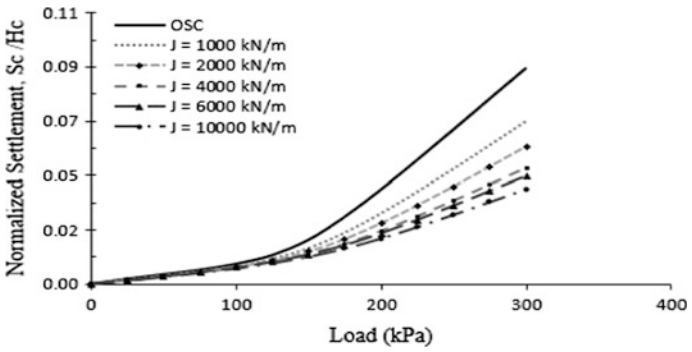


**Fig. 17** Effect of encasement on global stiffness of GECs-clay composite ground

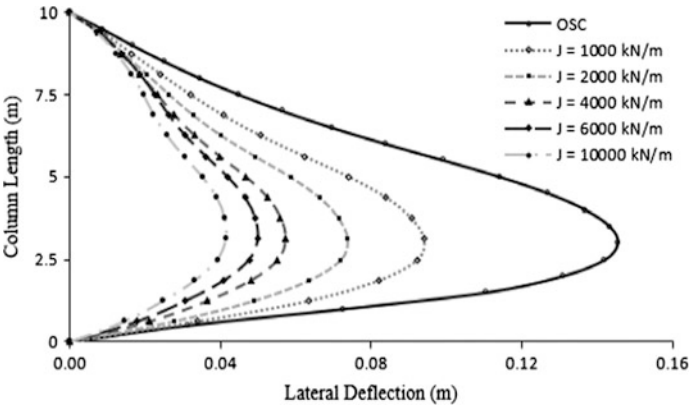


**Fig. 18** Lateral deflections of stone column 6 obtained from models with various encasement stiffnesses

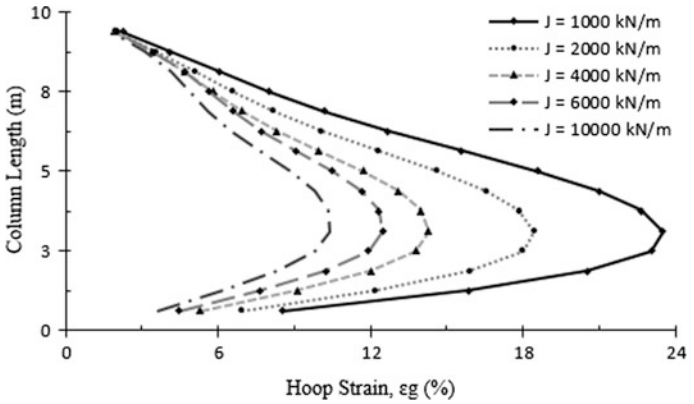


**Fig. 19** Geosynthetic hoop strain of stone column 6 obtained from models with various encasement stiffness

stiffness. In Fig. 18, it can be seen that lateral deflection of the stone column tends to sharply increase with length, by up to 145 mm at $3.5D_{sc}$, where $D_{sc}$ = stone column diameter, after which it decreases with length when no encasement is provided. This is attributed to mobilization of more load on top of the GECs (Fig. 14), and the subsequent transmission of greater loads to higher depths in the case of the GECs.

The geosynthetic hoop strain ($\varepsilon_g$) profiles, shown in Fig. 19, tend to follow the general trend observed in the $\delta_h$ profiles with a tendency of decreasing $\varepsilon_g$ with increasing $J$, showing a maximum hoop strain of 23.5% occurring at $3.5D_{sc}$ below the top of the stone column for $J$ = 1000 kN/M.

The confining effect provided by the geosynthetic encasement can be quantified using the ring tension force ($\Delta F_r$) developed in the geosynthetic encasement. The ring tension force can be expressed as $\Delta F_r = J \cdot \varepsilon_g$ where $\varepsilon_g$ = hoop strain, when assuming linear-elastic material behavior with stiffness $J$. The additional confining stress provided by the geosynthetic encasement $\Delta\sigma_{h,geo}$ can then be computed as $\Delta\sigma_{h,geo} = \Delta F_r / r_{geo}$ where $r_{geo}$ = radius of the encasement [28]. Substituting $\Delta F_r = J \cdot \varepsilon_g$ into $\Delta\sigma_{h,geo} = \Delta F_r / r_{geo}$ yields

$$\Delta\sigma_{h,geo} = \frac{J \cdot \varepsilon_g}{r_{geo}} \tag{1}$$

Figures 20 and 21 show $\Delta\sigma_{h,geo}$ profiles along the stone column for various cases, computed using the results of FE analyses together with Eq. (2) for a 300 kPa surcharge pressure. As one would expect, it can be seen in Fig. 20 that a stiffer encasement provides greater $\Delta\sigma_{h,geo}$, showing $(\Delta\sigma_{h,geo})_{max}$ = 500–2600 kPa

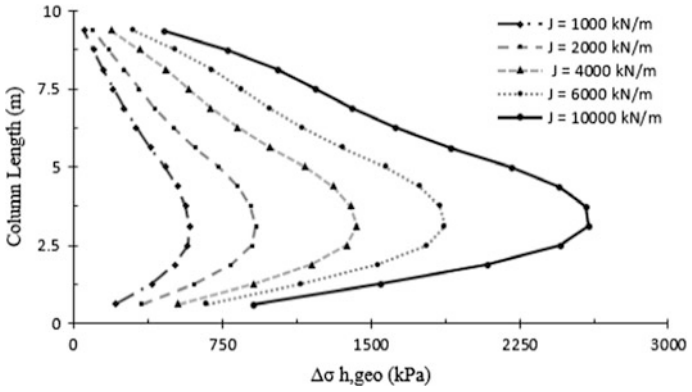


**Fig. 20** Variation of $\Delta\sigma_{h,geo}$ with influencing factors: effect of $J$

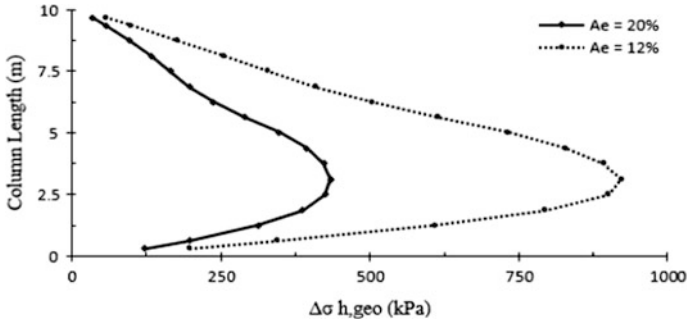


**Fig. 21** Variation of $\Delta\sigma_{h,geo}$ with influencing factors: effects of $a_E$

depending on $J$. Figure 21 also indicates that the confining stress provided by the encasement depends on the encasement stiffness. For example, as shown in Fig. 21, for $J$ = 2000 kN/M, larger $\Delta\sigma_{h,\text{geo}}$ are developed when the area replacement ratio $a_E$ is lower and/or the ground is weaker, showing $(\Delta\sigma_{h,\text{geo}})_{\max}$ = 920 kPa for $a_E$ = 10% as opposed to $(\Delta\sigma_{h,\text{geo}})_{\max}$ = 434 kPa for $a_E$ = 20%, depending on the soil consistency. These results in fact suggest that the encasement has a greater impact when $a_E$ is smaller, i.e., a lager spacing of GECs is weaker.

## 4.5 *Effect of Encasement Stiffness the GECs Performance*

The encasement stiffness $J$ is important design item as they directly affect the cost of GECs. The effects of $J$ on the GECs performance are examined. Figure 22 presents the variations of settlement ratio β with the encasement stiffness for GECs with $a_E$ = 12, 20% for a 300 kPa surcharge pressure. As one would expect, it can be seen that in all cases the settlement ratio β decreases rapidly with $J$ up to $J$ = 2000 KN/M after which it decreases at a decreased rate. Another trend shown in these figs is that the $\beta - J$ relationships are practically the same for a given area replacement ratio.

## 4.6 *Stiffness Improvement Factor*

Figure 23 shows the variations of stiffness improvement factor (SIF), defined as the ratio of the stiffness of GECs-reinforced ground ($K_{\text{GECs}}$) to that of untreated ground ($K_{\text{untreated}}$), with the encasement stiffness and the area replacement ratio. Note that the stiffness values of the GECs-reinforced and untreated ground, i.e., $K_{\text{GECs}}$, and $K_{\text{untreated}}$ are obtained from the respective $P_{\text{sur}} - S_c/H_c$ curves given in Fig. 16 as

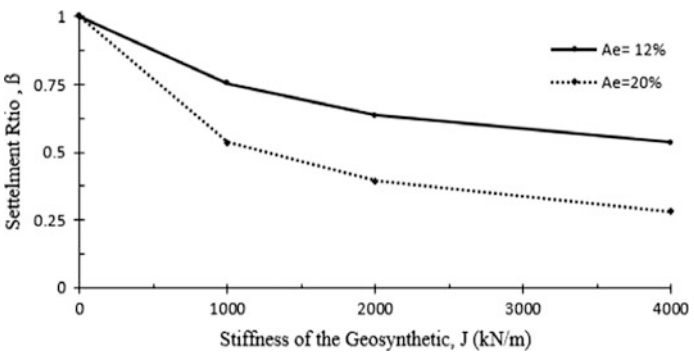


**Fig. 22** Variation of settlement ratio with of geosynthetic tensile stiffness

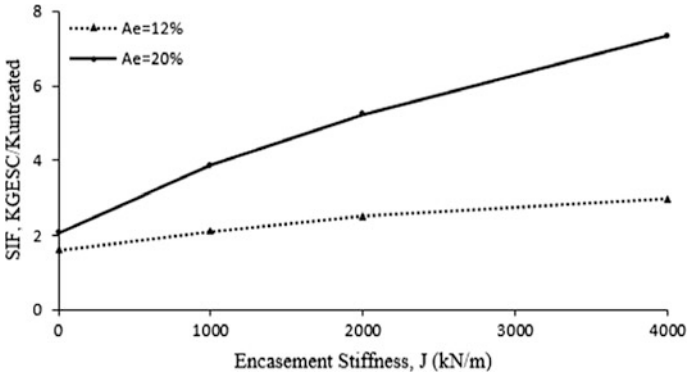


**Fig. 23** Variation of SIF with $J$ and $a_F$

average slopes. As shown, an eightfold increase in the stiffness of the ground can be achieved for the GECs with $J$ = 4000 kN/M and $a_E$ = 20% compared to that of the untreated ground. As before, cases with larger column spacing tend to yield greater SIF values for a given encasement stiffness, supporting the trend observed earlier.

Figure 23 can be used to make a preliminary estimate of the settlement of GECs-reinforced ground. For example, the settlement of GECs-reinforced ground $(S_c/H_c)_{GECs}$ under a given surcharge $P_{sur}$ can be obtained using the settlement of untreated ground $(S_c/H_c)_{untreated}$ and the SIF given in Fig. 20, since SIF can be written, by definition, as

$$\mathrm{SIF} = \frac{K_{GESC}}{K_{untreated}} = \frac{[p_{sur}/(S/H_c)]_{GESC}}{[P_{sur}/(S/H_c)]_{untreated}} = \frac{(S/H_c)_{untreated}}{(S/H_c)_{GESC}} a_F \tag{2}$$

The settlement of GECs-reinforced ground $(S_c/H_c)_{GECs}$ under a given embankment surcharge $P_{sur}$ can then be expressed as

$$\left(\frac{S}{H_c}\right)_{GESC} = \frac{1}{\mathrm{SIF}} \cdot \left(\frac{S}{H_c}\right)_{untreated} \tag{3}$$

Since $(S_c/H_c)$ untreated can be computed as $(S_c/H_c)$ untreated = $m_y \cdot \Delta\sigma'$, where $m_v$ = coefficient of volume compressibility of untreated ground and $\Delta\sigma'$ = effective stress increase, $(S_c/H_c)_{GECs}$ can be computed as $(S_c/H_c)$ GECs $= m_y.p_{sur}/\mathrm{SIF}$ assuming a constant $mv$ and $\Delta\sigma' = p_{sur}$.

## 5 Stress Concentration Ratio

The SCR versus normalized surcharge pressure $p_{sur}/E_{imp}$ relationships are shown in Figs. 24. Note that the normalized surcharge pressure,$p_{sur}/E_{imp}$ is used in this

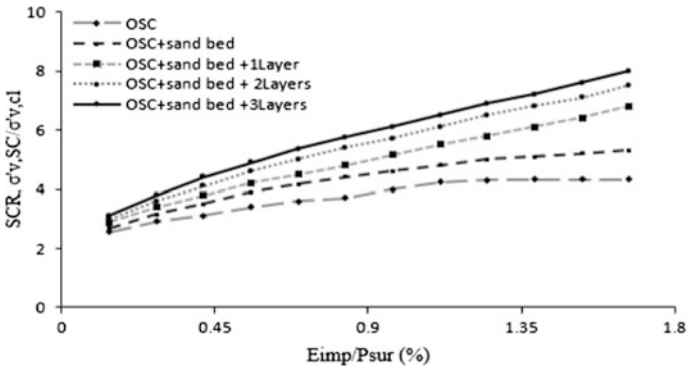


**Fig. 24** Variation of stress concentration ratio with surcharge pressure for multilayer geosynthetic-reinforced system

figure, where $E_{\text{imp}}$ = elastic modulus of the stone column-soil composite ground, computed based on the area replacement ratio as

$$E_{\text{imp}} = (A_{\text{s}} + A_{\text{sc}}) = E_{\text{sc}}A_{\text{sc}} + E_{\text{s}}A_{\text{s}}, \tag{4}$$

where $A_{\text{SC}}$ and $A_{\text{S}}$ are the surrounding soil and the cross-section areas of the stone column, respectively, and $E_{\text{sc}}$ and $E_{\text{s}}$ are the surrounding soil and elastic moduli of the stone column, respectively. Note that the elastic moduli of the untreated soils are computed using the following as:

$$E_{\text{s}} = \frac{3(1-2v)(1+e_0)p'}{k}, \tag{5}$$

where $p'$ = mean effective stress.

Figure 24 shows variation of stress concentration ratio with surcharge pressure for multilayer geosynthetic-reinforced sand bed with 40 cm thick placed over stone column. It can be seen, changes in the vertical effective stresses both in the stone column and in the clay layer caused by the multilayer geosynthetic-reinforced result in eight times larger SCR values for the three layers of geosynthetics-reinforcement than that for the OSC. The multilayer of geosynthetics-reinforcement transfers the stress from soil to stone columns due to stiffness difference between the soft soil and stone columns which reduce the possibility of soil yielding above stone columns. Thus, it can be said that there is a large increase in the values of stress concentration ratio in comparison to the values with the presence of geosynthetics-reinforcement when there is no geosynthetics-reinforcement present.

These changes in the vertical effective stresses both in the stone column and in the clay layer caused by the encasement result in nine times larger SCR values for the GECs with $J$ = 10,000 kN/M than that for the OSCs as shown in Fig. 25. The SCR tends to increase with the surcharge pressure load. Thus, it can be said

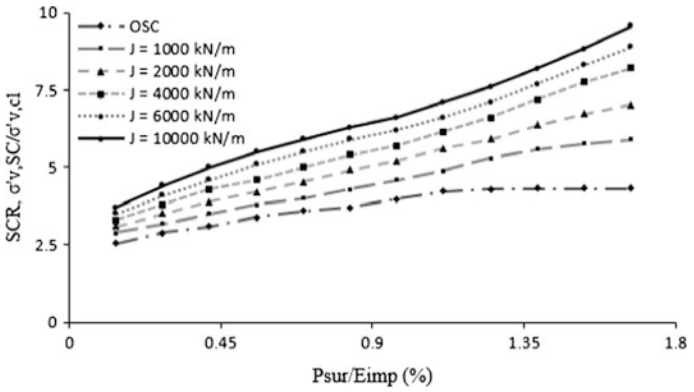


**Fig. 25** Variation of SCR with surcharge pressure at depth 2.5 m for GECs with various encasement stiffness

that use of GECs with an increase in the encasement tensile stiffness helps the stress transfer process and causes further reduction of stress on the soft soil.

## 6 Conclusions

In this paper, three-dimensional numerical analyses were performed to study the settlement response of multilayer geosynthetic-reinforced granular fill over stone column-reinforced soil. Finite-Element Analyses were carried out to compare the group performance of GECs with OSCs.

A detailed study was implemented to better understand the mechanism of load-carrying capacity in a group of GECs and OCSs. Based on the results gained from present research, the following conclusions can be found:

It has been observed that the use of multilayer geosynthetics-reinforcement with stone columns is not very effective to reduce the maximum settlement. The multilayer-reinforced system is very much effective to reduce the maximum settlement when stone columns are not provided in the soft soil. However, single-layer reinforcement with stone columns is very effective to reduce the maximum settlement.

The optimum thickness of geosynthetic-reinforced sand bed is 0.3 times the diameter of the footing. Decreases in bulge diameter in depth of bulge have been observed due to placement of sand bed over stone column-improved soft clay. Further decrease in maximum bulge diameter and increase in depth of bulge have been observed due to application of geosynthetic.

More stress concentration means more stress is transferred from soil to stone columns due to stiffness difference which helps to reduce the possibility of soil yielding above the stone columns. The use of geosynthetic reinforcements

significantly helps the stress transfer process and causes further reduction of stress on the soft soil.

When encasing the stone column, the lateral bulging is considerably decreased due primarily to the added confinement by the encasement. The confinement stresses inferred from the ring tension force developed in the geosynthetic encasement are larger when the area replacement ratio is smaller.

Increase in the stiffness of the geosynthetic encasement of the stone columns leads to increasing the column stiffness, the hoop tension force mobilized in the encasement, and the lateral confinement provided to the column, leading to substantial enhancement in the performance of the GECs group.

The critical geosynthetic encasement stiffness, beyond which no further benefit can be achieved, was found to be approximately $J = 2000$ KN/M and it appears to be independent of the area replacement ratio and the surcharge pressure load intensity for the conditions analyzed.

Encasing stone columns increased the end-bearing capacity. Encasement also allowed for greater load transfer to deeper depths, which was led to corresponding increases in loads that were transferred to the tip of the column.

## References

1. Hughes, J., Withers, N., Greenwood, D.: A field trial of the reinforcing effect of a stone column in soil. Geotechnique **25**, 31–44 (1975)
2. Madhav, M., Vitkar, P.: Strip footing on weak clay stabilized with a granular trench or pile. Can. Geotech. J. **15**, 605–609 (1978)
3. Aboshi, H., Ichimoto, E., Enoki, M., Harada, K.: The compozer—a method to improve characteristics of soft clays by inclusion of large diameter sand columns. Proc. Int. Conf. Soil Reinforcement ENPC **1**, 211–216 (1979)
4. Madhav, M., Miura, N.: Stone columns. In: Proceedings of the International Conference on Soil Mechanics and Foundation Engineering-International Society for Soil Mechanics and Foundation Engineering, pp. 163–163 (1994)
5. Deb, K.: Modeling of granular bed-stone column-improved soft soil. Int. J. Numer. Anal. Meth. Geomech. **32**, 1267–1288 (2008)
6. Deb, K.: Soil-structure interaction analysis of beams resting on multilayered geosynthetic-reinforced soil. Interact. Multiscale Mech. **5**, 369–383 (2012)
7. Han, J., Ye, S.-L.: Simplified method for consolidation rate of stone column reinforced foundations. J. Geotech. Geoenviron. Eng. **127**, 597–603 (2001)
8. Han, J., Gabr, M.: Numerical analysis of geosynthetic-reinforced and pile-supported earth platforms over soft soil. J. Geotech. Geoenviron. Eng. **128**, 44–53 (2002)
9. Van Impe, W.F.: Soil Improvement Techniques and Their Evolution (1989)
10. Malarvizhi, S., Ilamparuthi, K.: Load versus settlement of clay bed stabilized with stone and reinforced stone columns. In: Proceedingns of GeoAsia–2004, Seoul, Korea, pp. 322–329 (2004)
11. Ayadat, T., Hanna, A.: Encapsulated stone columns as a soil improvement technique for collapsible soil. Proc. Inst. Civ. Eng. Ground Improv. **9**, 137–147 (2005)
12. Murugesan, S., Rajagopal, K.: Geosynthetic-encased stone columns: numerical evaluation. Geotext. Geomembr. **24**, 349–358 (2006)

13. Gniel, J., Bouazza, A.: Improvement of soft soils using geogrid encased stone columns. Geotext. Geomembr. **27**, 167–175 (2009)
14. Khabbazian, M., Kaliakin, V.N., Meehan, C.L.: 3D numerical analyses of geosynthetic encased stone columns. In: 2009 International Foundation Congress and Equipment Expo (2009)
15. Kempfert, H., Göbel, C., Alexiew, D., Heitz, C.: German recommendations for reinforced embankments on pile-similar elements. In EuroGeo3-Third European Geosynthetics Conference, Geotechnical Engineering with Geosynthetics, pp. 279–284 (2004)
16. Deb, K., Basudhar, P., Chandra, S.: Generalized model for geosynthetic-reinforced granular fill-soft soil with stone columns. Int. J. Geomech. **7**, 266–276 (2007)
17. Deb, K., Samadhiya, N.K., Namdeo, J.B.: Laboratory model studies on unreinforced and geogrid-reinforced sand bed over stone column-improved soft clay. Geotext. Geomembr. **29**, 190–196 (2011)
18. Ambily, A., Gandhi, S.R.: Behavior of stone columns based on experimental and FEM analysis. J. Geotech. Geoenviron. Eng. **133**, 405–415 (2007)
19. Deb, K., Sivakugan, N., Chandra, S., Basudhar, P.: Numerical analysis of multi layer geosynthetic-reinforced granular bed over soft fill. Geotech. Geol. Eng. **25**, 639–646 (2007)
20. Yoo, C.: Performance of geosynthetic-encased stone columns in embankment construction: numerical investigation. J. Geotech. Geoenviron. Eng. **136**, 1148–1160 (2010)
21. Liu, H., Ng, C.W., Fei, K.: Performance of a geogrid-reinforced and pile-supported highway embankment over soft clay: case study. J. Geotech. Geoenviron. Eng. **133**, 1483–1493 (2007)
22. Alexiew, D., Brokemper, D., Lothspeich, S.: Geotextile encased columns (GEC): load capacity, geotextile selection and pre-design graphs. In: Proceeding of the Geo-Frontiers 2005 Congress, Austin, Texas, pp. 1–14 (2005)
23. Barksdale, R., Bachus, R.: Design and Construction of Stone Columns, Appendixes, vol. II. Federal Highway Administration, Washington DC, USA (1983)
24. Shahu, J., Madhav, M., Hayashi, S.: Analysis of soft ground-granular pile-granular mat system. Comput. Geotech. **27**, 45–62 (2000)
25. Basudhar, P., Dixit, P., Gharpure, A., Deb, K.: Finite element analysis of geotextile-reinforced sand-bed subjected to strip loading. Geotext. Geomembr. **26**, 91–99 (2008)
26. Burd, H.: Analysis of membrane action in reinforced unpaved roads. Can. Geotech. J. **32**, 946–956 (1995)
27. Lee, K., Manjunath, V., Dewaikar, D.: Numerical and model studies of strip footing supported by a reinforced granular fill-soft soil system. Can. Geotech. J. **36**, 793–806 (1999)
28. Raithel, M., Kempfert, H.-G.: Calculation models for dam foundations with geotextile coated sand columns. In: ISRM International Symposium (2000)